Environ. Sci. Technol. **2002**, *36,* 4081−4086

Kinetic and Mechanistic Study of the Atmospheric Oxidation by OH Radicals of Allyl Acetate

B. PICQUET-VARRAULT,* J.-F. DOUSSIN, R. DURAND-JOLIBOIS, O. PIRALI, AND P. CARLIER

Laboratoire Interuniversitaire des Systèmes Atmosphériques, UMR-CNRS 7583, Universités de Paris 7 et Paris 12, 61 Avenue du Général de Gaulle, 94010 Créteil Cedex, France

C. FITTSCHEN

Laboratoire de Cinétique et Chimie de la Combustion, UMR-CNRS 8522, Université des Sciences et Technologies de Lille, Bat. C11, 59655 Villeneuve d'Ascq Cedex, France

Acetates are emitted into the atmosphere by several anthropic and natural sources. To better evaluate the environmental impact of these compounds, OH-induced oxidation kinetic and mechanism of allyl acetate ($CH_3C(O)OCH_2$-$CH{=}CH_2$) have been investigated at room temperature and atmospheric pressure using three environmental chambers: an indoor Teflon-film bag (LISA, Créteil), an indoor Pyrex photoreactor (LISA, Créteil), and the outdoor Smog chamber EUPHORE (Valencia). Rate constant of the reaction of allyl acetate with OH radicals was determined by relative rate technique in the indoor Teflon-film bag. It is $(30.6 \pm 3.1) \times 10^{-12}$ cm^3 molecule^{-1} s^{-1}. Mechanistic experiments were performed in the indoor photoreactor and in the outdoor Smog chamber EUPHORE. The main oxidation products observed by FTIR in both chambers were acetoxyacetaldehyde and formaldehyde. From these data, a mechanism was developed to describe the OH-induced oxidation of this acetate in the presence of NOx. Finally, atmospheric impact of allyl acetate emissions was evaluated using kinetic and mechanistic results.

1. Introduction

Acetates have been widely released for decades into the atmosphere during their use in industrial activities. Moreover, they are also emitted from natural sources (vegetation and biomass combustion) (*1*). An additional potential source of these compounds, including allyl acetate ($CH_3C(O)OCH_2$-$CH{=}CH_2$), is combustion of esterified rape oil used as substitution fuel (*2*). This new formulation of diesel fuel significantly reduces the emission of particulate matter (*2*, *3*), but aldehydes and esters emissions are increased (*2*). When released into the atmosphere, these oxygenated compounds can undergo photochemical transformations which can lead to the production of ozone and other photooxidants. To evaluate the potential impact on health and environment of a massive use of this substitution fuel, a precise knowledge of the atmospheric oxidation of acetates by OH radicals is needed as this process is their main daytime fate. Few previous kinetic studies have already been carried out for allyl acetate (*4*−*6*), but no mechanistic data have been published yet. The present study is focused on the oxidation of allyl acetate.

2. Experimental Section

Experiments were performed using three environmental chambers: an indoor Teflon-film bag (LISA, Créteil), an indoor Pyrex photoreactor (LISA, Créteil), and the outdoor Smog chamber EUPHORE (Valencia). These three photoreactors are briefly presented here.

2.1. Indoor Teflon-Film Bag. All kinetic experiments were performed using a Teflon-film bag of approximately 250 L surrounded by three sets of fluorescent tubes (10 tubes Philips TUV15, 18 Philips TL05, and 18 Philips TL03). The emissions of these "black lamps" are respectively centered on 254, 360, and 420 nm. Hydroxyl radicals were generated by photolyzing hydrogen peroxide. Concentrations of selected reactants were in the ppm range in purified air (Section Chemicals and gases) and were recorded by gas chromatography using a Carlo Erba gas chromatograph GC 6000 Vega Series 2 equipped with a Megabore DB 225 column (30 m × 0.53 mm, film thickness: 1 μm) and a flame ionization detector.

2.2. Indoor Evacuable Photoreactor. Mechanistic study was mainly carried out in an evacuable environmental chamber comprising a Pyrex reactor of 977 L surrounded by two sets of 40 fluorescent tubes (Philips TL05 and TL03). The emissions of these black lamps are respectively centered on 360 and 420 nm. Moreover,16 arc lamps (Osram, 400 W) provide an irradiation with a broad spectral range from 360 to 600 nm. The reactor contains a multiple reflection optical system interfaced to a FTIR spectrometer (BOMEM DA8-ME). Details of this environmental chamber are given by Doussin et al. (*7*). Hydroxyl radicals were generated by photolyzing methyl nitrite or nitrous acid. The initial concentrations of the reactants (acetate, methyl nitrite, and NO) were in the ppm range in a synthetic mixture of 80% N_2 and 20% O_2 (NO was added to limit formation of nitrate radicals and ozone). All experiments were conducted at 298 ± 5 K with continuous irradiation during 1 or 2 h. Compounds were monitored by acquiring infrared spectra every 4 min (corresponding to 100 co-added interferograms) with a resolution of 0.7 cm^{-1} and a path length of 96 or 186 m.

2.3. Outdoor Smog Chamber EUPHORE. Additional mechanistic experiments were carried out in the outdoor simulation chamber EUPHORE in Valencia (Spain). The chamber is made of a half-spherical 204 m^3 Teflon-film bag submitted to sunlight irradiation. The reactor contains a multiple reflection optical system interfaced to a FTIR spectrometer (Nicolet Magna 550). Details of this chamber are given by Becker et al. (*8*). Hydroxyl radicals were generated by photolyzing nitrous acid which was formed in the chamber by reaction of NOx with water adsorbed on the walls of the reactor. Typical initial concentrations were 1 ppm acetate and ∼100 ppb NO in purified air. All experiments were conducted at 303 ± 3 K with continuous solar irradiation during approximately 3 h. Compounds were monitored by acquiring infrared spectra every 5 min (corresponding to 250 co-added interferograms) with a resolution of 1 cm^{-1} and a path length of 553.5 m.

A slight excess of pressure in the chamber is necessary to stabilize the Teflon bag against the wind. Therefore, to counteract the loss due to slight leaks, small amounts of dried air are periodically introduced in the chamber and cause small dilution of the mixtures. The dilution rate τ was determined by introducing an inert dilution tracer (SF_6) and

* Corresponding author phone: (33) 1 45 17 15 90; fax: (33) 1 45 17 15 64; e-mail: picquet@lisa.univ-paris12.fr.

10.1021/es0200138 CCC: $22.00
Published on Web 09/04/2002

by following its concentration during the experiments by FTIR.

2.4. Relative Rate Technique. Relative rate technique was used to determine the rate constant of the OH-induced oxidation of allyl acetate. Since this method has already been described numerous times (*9*), we only present briefly its principle here. If the reaction with OH is the only fate of the studied compound (X) and of the reference compound (R) and if no secondary reaction occurs

$$X + OH \rightarrow \text{products} \quad k_X$$

$$R + OH \rightarrow \text{products} \quad k_R$$

it can be shown that

$$\ln \frac{[X]_0}{[X]_t} = \frac{k_X}{k_R} \ln \frac{[R]_0}{[R]_t}$$

where $[X]_0$ and $[R]_0$ and $[X]_t$ and $[R]_t$ are, respectively, the concentrations of the selected compound and the reference compound at times 0 and t. A plot of $\ln([X]_0/[X]_t)$ vs $\ln([R]_0/[R]_t)$ yields a straight line with a slope of k_X/k_R and an intercept of zero. The uncertainty on this value was determined using the software developed by Brauers and Finlayson-Pitts (*10*). This method performs linear regressions of the plots of $\ln([X]_0/[X]_t)$ vs $\ln([R]_0/[R]_t)$ by taking into account errors in both [R] and [X].

The kinetic experiments were performed at 298 ± 4 K and at atmospheric pressure using H_2O_2 as OH precursor and *n*-octane as reference compound ($k_{n\text{-octane} + OH} = 8.71 \times 10^{-12}$ cm^3 molecule^{-1} s^{-1} (*11*)). To verify that none of the reference nor the studied compounds were photolyzed at our experimental conditions, these compounds were irradiated approximately 2 h (twice the duration of a kinetic experiment). No significant loss was observed.

2.5. Determination of the Formation Yields of Oxidation Products. For experiments carried out in the indoor photoreactor at LISA, formation yields of oxidation products were determined by calculating the initial slopes of the curves [products] vs $-\Delta$[allyl acetate]. In EUPHORE, since the mixtures are subject to dilution during the experiments, formation yields were calculated as follows: assuming the reaction

$$A + OH \rightarrow B \quad \alpha k$$

where α is the formation yield of B and k is the global rate constant of the oxidation of A by OH.

$$\frac{d[A]}{dt} = -\tau[A] - k[A][OH] \Rightarrow$$

$$\alpha \frac{d[A]}{dt} = -\alpha\tau[A] - \alpha k[A][OH]$$

and

$$\frac{d[B]}{dt} = -\tau[B] + \alpha k[A][OH]$$

From these equations, we can deduce that

$$\alpha = -\frac{\frac{d[B]}{dt} + \tau[B]}{\frac{d[A]}{dt} + \tau[A]}$$

τ is calculated for each experiment using the dilution tracer. It is commonly between 5×10^{-6} and 7×10^{-6} s^{-1}.

TABLE 1. Integrated Band Intensities of the Main Infrared Absorption Bands of Allyl Acetate and Its Oxidation Products

compound	main absorption band/cm^{-1}	IBI/cm molecule^{-1}	ref
allyl acetate	1325−1155	$(5.64 \pm 0.18) \times 10^{-17}$	this work
acetoxyacetaldehyde	1300−1170	$(3.2 \pm 0.6) \times 10^{-17}$	this work
formaldehyde	3000−2630	$(3.03 \pm 0.13) \times 10^{-17}$	this work
formic acetic anhydride	1095−1005	$(5.99 \pm 0.13) \times 10^{-17}$	this work
acetic acid	1840−1712	$(4.36 \pm 0.24) \times 10^{-17}$	this work

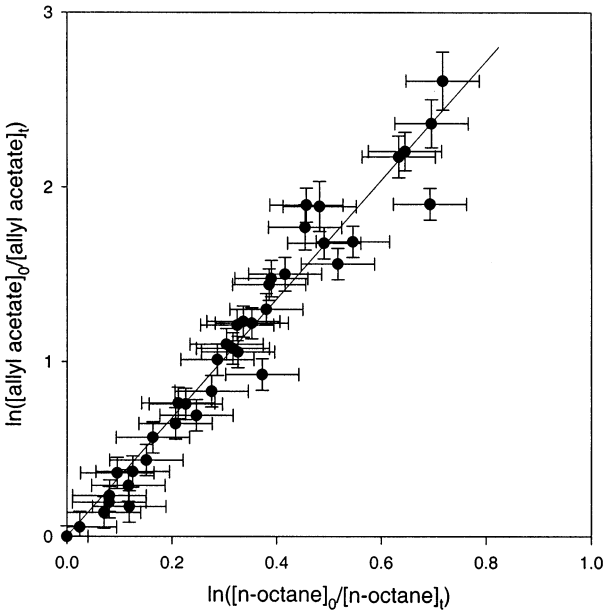

FIGURE 1. Plot of the kinetic data for the reaction of OH radicals with allyl acetate vs *n*-octane.

TABLE 2. OH Reaction Rate Constant of Allyl Acetate—Comparison with Previous Data

reactant	$k \times 10^{12}$ cm^3 molecule^{-1} s^{-1}	technique	ref
allyl acetate	30.6 ± 3.1	RR (*n*-octane)	this work
	24.57 ± 0.24	RR (*n*-octane)	Ferrari et al. (*4*)
	27.1 ± 3.0	LP-LIF	Le Calvé et al. (*6*)
	28.9 ± 4.5	RR (propene)	Le Calvé (*5*)

For both sets of experiments, indicated errors of yields take into account the estimated uncertainties in reactant and products IR absorption bands calibrations (see Table 1) and the uncertainties in the calculation of yields. Errors due to the calculation of yields are two standard deviations on the calculation of α at EUPHORE and two standard deviations of the initial slope of the curve [product] vs $-\Delta$[acetate] in the indoor photoreactor. Errors due to the quantification of compounds in infrared spectra have been disregarded because they are not significant compared to the previous ones.

2.6. Chemicals and Gases. Methyl nitrite used as OH precursor was prepared by slowly adding a dilute solution of H_2SO_4 to a mixture of $NaNO_2$ and methanol (*12*). Nitrous acid was synthesized by slowly adding a dilute solution of $NaNO_2$ to diluted H_2SO_4 (*13*). Methyl nitrate, formic acetic anhydride, and acetoxyacetaldehyde which were supposed to be oxidation products of allyl acetate were also synthesized (*14*). Other organic reagents were obtained from commercial sources: allyl acetate was from Aldrich (99%) and acetic acid was from Prolabo (≥ 99%). Synthetic air used to fill the indoor

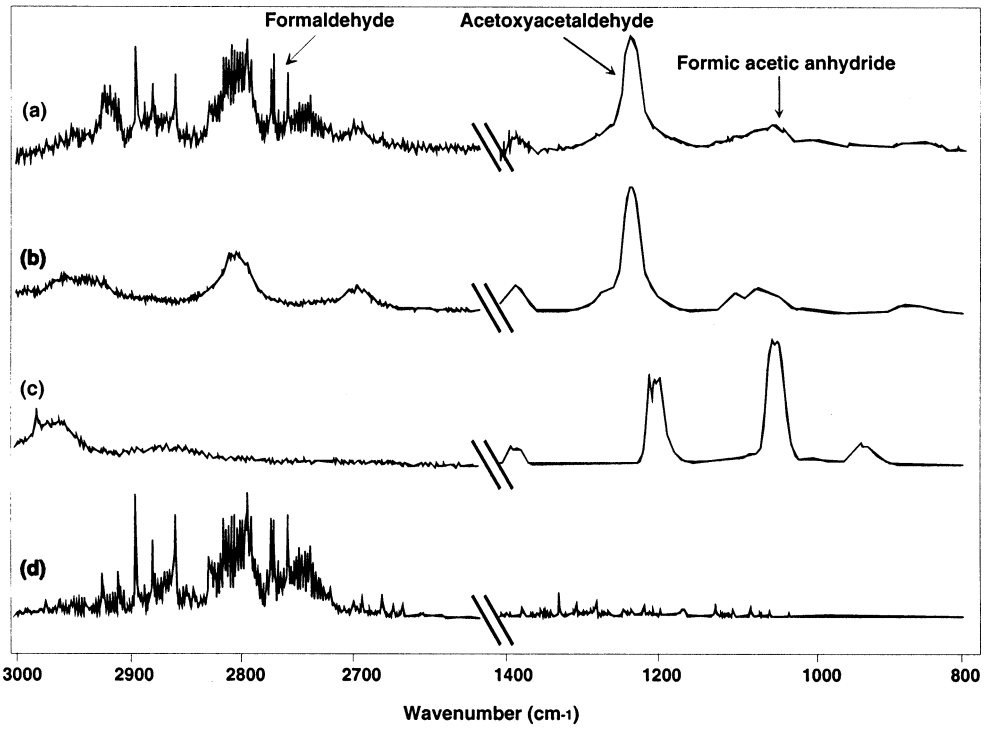

FIGURE 2. Residual infrared spectrum obtained after the photolysis of HONO/allyl acetate mixture: (a) residual spectrum obtained by subtraction of remaining reactants, compared with reference spectra of acetoxyacetaldehyde (b), formic acetic anhydride (c), and formaldehyde (d).

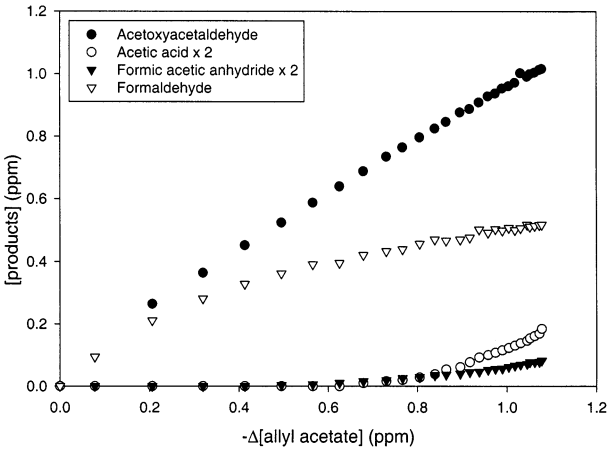

FIGURE 3. Experimental plots of the formation of oxidation products vs loss of allyl acetate, obtained at LISA.

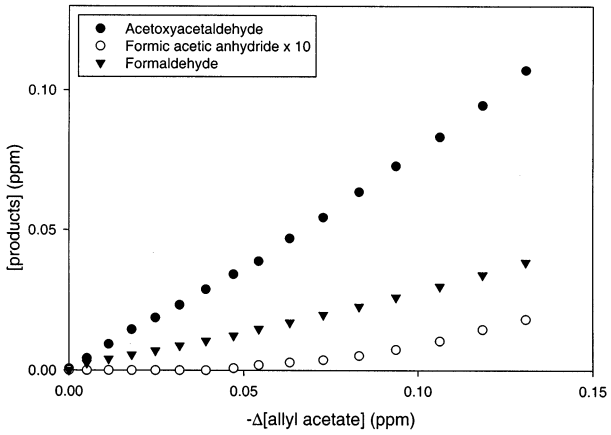

FIGURE 4. Experimental plots of the formation of oxidation products vs loss of allyl acetate, obtained at EUPHORE.

evacuable photoreactor (LISA) was generated using O_2 (quality N45, ≥ 99.99%, Air Liquide) and N_2 (from liquid nitrogen evaporation, ≥ 99.995%, Linde). The air used in the Teflon-film bag was purified through cartridges filled with silicagel, soda lime, vegetal charcoal and molecular sieve. The experiments in EUPHORE reactor were also performed in dried and purified air (*8*).

Results and Discussion

3.1. Relative Rate Study. To determine the rate constant of the reaction of allyl acetate with OH radicals, *n*-octane, allyl acetate, and H_2O_2 were introduced into the dark chamber. Organic reactants concentrations were between 1 and 2 ppm. Several samples of gases were taken to accurately determine the initial amount of each organic reactant. Then the bag was irradiated continuously for approximately 1 h and samplings were performed at short and steady time intervals (~5 min). From the amounts of allyl acetate and *n*-octane measured during the experiments, $\ln([\text{allyl acetate}]_0/[\text{allyl acetate}]_t)$ vs $\ln([n\text{-octane}]_0/[n\text{-octane}]_t)$ was plotted (see Figure 1).

The rate constant was found equal to $(30.6 \pm 3.1) \times 10^{-12}$ cm^3 $molecule^{-1}$ s^{-1} and was compared to previous data in Table 2. From these data, we can see that the value of the rate constant obtained in this study is in good agreement with those of Le Calvé et al. (*5*, *6*) obtained by absolute and relative rate determinations and that the value of Ferrari et al. (*4*) is slightly lower than ours. Ferrari et al. used a rate constant for the reaction of OH radicals with *n*-octane (their reference compound) equal to 8.42×10^{-12} cm^3 $molecule^{-1}$ s^{-1} whereas this study used 8.71×10^{-12} cm^3 $molecule^{-1}$ s^{-1} (*11*) for the same reference compound. By using this last value for the determination of Ferrari et al., $k_{\text{allyl acetate + OH}}$ was found equal to 25.4×10^{-12} cm^3 $molecule^{-1}$ s^{-1} and still be slightly different from ours. However, it can be seen that

SCHEME 1. Oxidation Scheme of Allyl Acetate Obtained from the Generally Accepted Process of VOC Oxidation and from Formation Yields of the Detected Products (Framed)

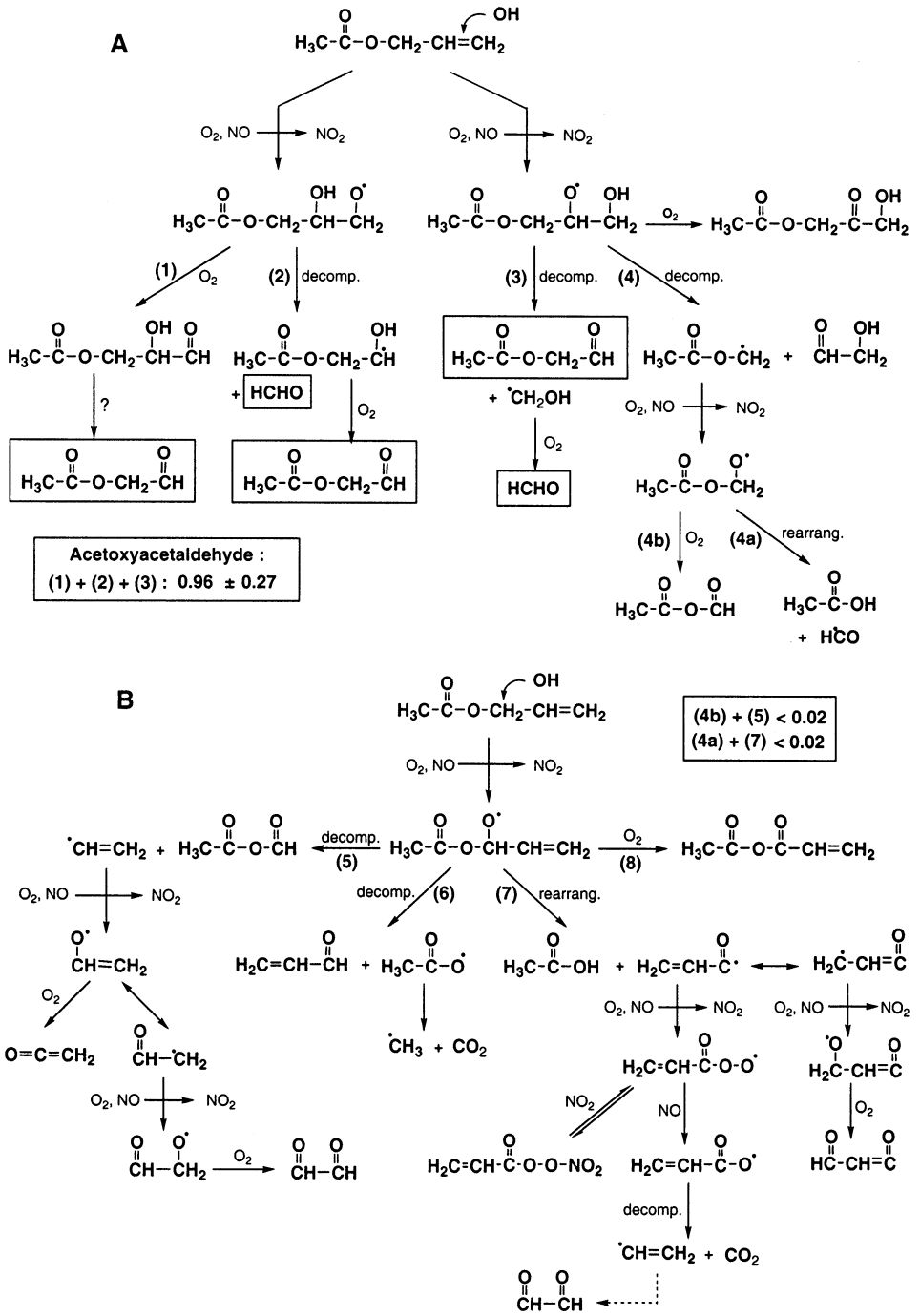

the uncertainties range given by these authors is very small (~1%) and may not take into account the errors in both [R] and [X]. Therefore, they may be underestimated. and we cannot really state that the difference between these values is significant.

3.2. Mechanistic Study. The mechanism of OH-induced oxidation of allyl acetate was investigated in the indoor environmental chamber by photolyzing CH_3ONO/allyl acetate/NOx and HONO/allyl acetate/NOx mixtures in the evacuable photoreactor. Acetate and NOx concentrations were close to 1 ppm. An additional experiment was carried out in the photoreactor EUPHORE by photolyzing allyl acetate/NOx mixture (1.2 ppm/100 ppb) in order to compare the results obtained under different experimental conditions (irradiation, NOx level, surface/volume ratio, ...). In both kinds of experiments, reactants and products were analyzed by FTIR spectrometry. Figure 2 shows an example of a residual spectrum acquired after ~5000 s of irradiation, obtained by subtraction of remaining reactants (allyl acetate, HONO, NO) and inorganic compounds. Remaining products which are attributed to oxidation of allyl acetate are acetoxyacetaldehyde, formic acetic anhydride, and formaldehyde. Small amounts of acetic acid have also been detected but its absorption bands are not visible on the scale of the figure.

Examples of the plots [products] vs $-\Delta$[allyl acetate] for an experiment carried out in the indoor reactor using HONO as OH source and for the experiment performed at EUPHORE are respectively shown in Figures 3 and 4. On these figures, it can be seen that acetoxyacetaldehyde and formaldehyde whose plots have initial slope different from zero are primary

SCHEME 2

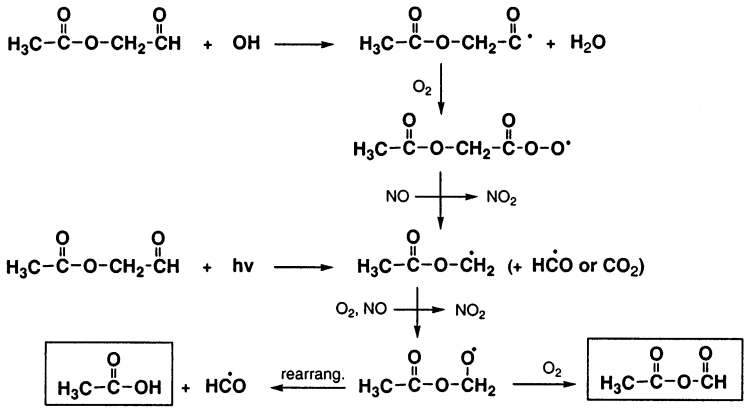

products whereas acetic acid and formic acetic anhydride are secondary products. Acetoxyacetaldehyde and formaldehyde which are the main oxidation products, can be formed by an addition of OH radicals on the double bond followed by a decomposition of the two alkoxy radicals formed: $CH_3C(O)OCH_2CH(OH)CH_2O^\bullet$ and/or $CH_3C(O)OCH_2CH(O^\bullet)$-$CH_2OH$ (see Scheme 1A, channels 2 and 3).

For the experiment performed at LISA, the decrease of the slopes indicates that formaldehyde and to a lesser extent, acetoxyacetaldehyde are subject to secondary loss processes: formaldehyde can react with OH and HO_2 radicals and can be photolyzed. Here, this last process is of minor importance since its photolysis constant in the indoor reactor was measured to be $\sim 2.5 \times 10^{-5}$ s^{-1} leading to a photolysis lifetime of formaldehyde of about 11 h. Acetoxyacetaldehyde may be photolyzed and may react with OH radicals (see Scheme 2). These two processes can lead to the formation of the $CH_3C(O)OCH_2O^\bullet$ radical which reacts with O_2 to form formic acetic anhydride or undergoes an α-ester rearrangement to form acetic acid (*15*).

At EUPHORE, no significant loss of acetoxyacetaldehyde and formaldehyde was observed but the plots are not very precise because of the dilution process in the chamber. Moreover, OH and HO_2 concentrations are smaller in the outdoor reactor than at LISA ([OH] $\sim 10^7$ molecule/cm^3 at LISA and [OH] $\sim 10^6$ molecule/cm^3 at EUPHORE) leading to a slighter secondary chemistry.

Since photolysis and OH-induced oxidation of acetoxyacetaldehyde have not been studied and since HO_2 concentrations cannot be precisely determined, the quantification of secondary processes involving acetoxyacetaldehyde and HCHO was not possible. Hence the curves [products] vs $-\Delta$[allyl acetate] were not corrected for secondary reactions. As a result, formation yields were determined using only the initial slopes of the curves. This method allows also for disregarding the reactions of allyl acetate with NO_3 and O_3 which have been found negligible during the first half-hour of the experiments. Hence, by comparing $k_{(\text{allyl acetate + OH})} \times$ [OH], $k_{(\text{allyl acetate + NO3})} \times [NO_3]$, and $k_{(\text{allyl acetate + O3})} \times [O_3]$, it was shown that during the first half-hour of the experiment, the chemistry induced by O_3 and the chemistry induced by NO_3 count for less than 5% compared to the reaction with OH. The rate constants used were $k_{(\text{allyl acetate + O3})} = 2.4 \times 10^{-18}$ cm^3 $molecule^{-1}$ s^{-1} (*6*) and 5×10^{-14} cm^3 $molecule^{-1}$ s^{-1} (estimation by Wayne et al. (*16*) and Sabljic et al. (*17*)). Since N_2O_5 was not detected during the experiments, the upper limit of NO_3 concentration was determined using the infrared detection limit of N_2O_5 and the equilibrium constant of the reaction $NO_2 + NO_3 \leftrightarrow N_2O_5$, 2.89×10^{-11} cm^3 $molecule^{-1}$ s^{-1} (*18*).

Final products yields are shown in Table 3. From these results, we observe that formation yields of acetoxyacetaldehyde obtained in the three experiments are in good agreement within the experimental uncertainties whereas those of formaldehyde are significantly different: the formaldehyde yield obtained in EUPHORE is much lower than those obtained in the indoor photoreactor. This experimental result may be related with the NOx level which was much lower in the EUPHORE chamber than in the indoor photoreactor (100 ppb and 1 ppm). Under high NO condition, the exothermic reactions of $CH_3C(O)OCH_2CH(OH)CH_2O_2^\bullet$ and $CH_3C(O)OCH_2CH(O_2^\bullet)CH_2OH$ radicals with NO may lead to excited alkoxy radicals: $CH_3C(O)OCH_2CH(OH)CH_2O^{\bullet *}$ and $CH_3C(O)OCH_2CH(O^{\bullet *})CH_2OH$. The fraction of excited alkoxy radicals would then be larger in the indoor photoreactor (at ≪ high NOx ≫) than at EUPHORE (at ≪ low NOx ≫), and these radicals would be more prone to decompose than those produced at lower NO level, in the less exothermic peroxy self-reaction. Therefore, a possible explanation of this observation is that excited $CH_3C(O)OCH_2CH(OH)CH_2O^{\bullet *}$ radicals would mainly decompose to form acetoxyacetaldehyde and formaldehyde, whereas nonexcited radicals would preferably react with O_2. The reaction with O_2 leads to the formation of $CH_3C(O)OCH_2CH(OH)CHO$ which might rapidly form acetoxyacetaldehyde and $HC^\bullet O$ (by decomposition, reaction with OH or photolysis ?). In conclusion, the decomposition of $CH_3C(O)OCH_2CH(OH)CH_2O^\bullet$ radicals would lead to acetoxyacetaldehyde + HCHO, whereas its reaction with O_2 would lead to acetoxyacetaldehyde only (see Scheme 1). This reaction scheme offers an explanation why the formaldehyde yield was lower in EUPHORE. It also explains that acetoxyacetaldehyde yield is slightly smaller in the experiment at ≪ low NOx ≫ since some peroxides may be produced from peroxy radical + HO_2 reaction and compete with the acetoxyacetaldehyde production. Similar chemical activation effects have already been reported in the literature for other alkoxy radicals when experiments were performed with and without NOx (*15*, *19*, *20*). Christensen et al. (*15*) who have studied the atmospheric oxidation of methyl acetate have shown that the decomposition branching ratio of $CH_3C(O)OCH_2O^\bullet$ radicals was higher in the presence of NOx than in absence of NOx.

TABLE 3. Oxidation Products of Allyl Acetate and Their Formation Yields

	indoor photoreactor		
product	acetate/ CH_3ONO/NOx	acetate/ HONO/NOx	EUPHORE acetate/NOx
acetoxyacetaldehyde	0.97 ± 0.25	1.00 ± 0.25	0.90 ± 0.24
formaldehyde	0.90 ± 0.15	0.97 ± 0.15	0.37 ± 0.08
formic acetic anhydride	<0.02	<0.02	<0.02
acetic acid	<0.02	<0.02	<0.02

Finally, according to FTIR detection limit of acetic acid and formic acetic anhydride, we can deduce that any primary formation of these two products would have a molar yield < 0.02. This observation confirms that OH radicals add to the double bond rather than abstracting a hydrogen atom. Unfortunately, since the addition on both carbons of the double bond leads to the same products, we cannot distinguish these two pathways.

4. Atmospheric Implications. In the atmosphere, allyl acetate can be removed by photolysis and by reactions with ozone, OH, and NO_3 radicals. In this study, kinetic and mechanism of its OH-induced oxidation have been investigated. The rate constant obtained is in good agreement with the few previous ones (*4*−*6*) and contributes to better predict the tropospheric lifetimes of this acetate. Hence, assuming a typical tropospheric OH concentration of 2×10^6 molecule cm^{-3}, the tropospheric daily lifetime of allyl acetate against reaction with OH was estimated to be 5 h. Using the experimental and estimated rate constants of allyl acetate toward NO_3 and O_3 (*6*, *16*, *17*) and typical tropospheric concentrations of these oxidants (15 ppt for NO_3 and 40 ppb for O_3), the corresponding lifetimes were 5 days for ozonolysis and 15 h for reaction with NO_3. Thus, it appears that reaction with OH radicals is the main tropospheric fate of allyl acetate. When it reacts with OH radicals, it may contribute to the formation of photooxidants close to the emission sources.

From the mechanistic study, main oxidation products of allyl acetate, acetoxyacetaldehyde, and formaldehyde were detected. Acetoxyacetaldehyde, like many aldehydes, may be photolyzed and may also be reactive toward OH radicals. From this study, we strongly suspect that these reactions lead to the formation of formic acetic anhydride and acetic acid, but these observations need to be confirmed with specific experiments on the oxidation processes of this product. Moreover, mechanistic studies on the oxidation of other acetates (*14*, *21*) have shown that acetoxyacetaldehyde was also significantly formed by these processes. Therefore, kinetic and mechanistic experiments on the chemistry of acetoxyacetaldehyde are needed to better evaluate the environmental impact of the emissions of acetates in the atmosphere.

Acknowledgments

We thank the French ministry of environment for supporting this research as part of PRIMEQUAL and PNCA programs. We acknowledge Klaus Wirtz and EUPHORE team for their cooperation. We also gratefully thank Prof. Françoise Heymans and her collaborators for their help in the synthesis of acetoxyacetaldehyde.

Literature Cited

(1) Graedel, T. E.; Hawkins, D. T.; Claxton, L. D. *Atmospheric Chemical compounds*: *Sources, Occurrence, and Bioassay;* Academic Press: Orlando, FL, 1986.
(2) Ferrari, C., Ph.D., Université Joseph Fourier-Grenoble 1, 1995.
(3) Guillaume, F. *Les biocarburants dans l'Union Européenne*; Assemblée Nationale, 2000.
(4) Ferrari, C.; Roche, A.; Jacob, V.; Foster, P.; Baussand, P. *Int. J. Chem. Kinet.* **1996**, *28*, 609.
(5) Le Calvé, S., Ph. D., Université d'Orléans, France, 1998.
(6) Le Calvé, S.; Mellouki, A.; Le Bras, G.; Treacy, J.; Wenger, J.; Sidebottom, H. *J. Atmos. Chem.* **2000**, *7*, 161.
(7) Doussin, J. F.; Ritz, D.; Durand-Jolibois, R.; Monod, A.; Carlier, P. *Analusis* **1997**, *25*, 236.
(8) Becker, K. H.; Hjorth, J.; Laverdet, G.; Millan, M. M.; Platt, U.; Toupance, G.; Wildt, J. *Design and Technical Development of the European Photoreactor and First Experimental Results;* EV5V-CT92-0059, 1996.
(9) Finlayson-Pitts, B.; Pitts, J. N., Jr. *Atmospheric Chemistry*: *Fundamentals and Experimental Techniques*; John Wiley and Sons: New York, 1986.
(10) Brauers, T.; Finlayson-Pitts, B. J. *Int. J. Chem. Kinet.* **1997**, *29*, 665.
(11) Atkinson, R. *J. Phys. Chem. Ref. Data* **1997**, *26*, 2, 216.
(12) Taylor, W. D.; Allston, T. D.; Moscato, M. J.; Fazenkas, G. B.; Koslowski, R.; Takacs, G. A. *Int. J. Chem. Kinet.* **1980**, *12*, 231.
(13) Nash, T. *Ann. Occup. Hyg.* **1968**, *11*, 235.
(14) Picquet-Varrault, B.; Doussin, J. F.; Durand-Jolibois, R.; Carlier, P. *Phys. Chem. Chem. Phys.* **2001**, *3*, 2595.
(15) Christensen, L. K.; Ball, J. C.; Wallington, T. J. *J. Phys. Chem. A* **2000**, *104*, 345.
(16) Wayne, R. P.; Barnes, I.; Biggs, P.; Burrows, J. P.; Casona-Mas, C. E.; Hjorth, J.; Le, B. G.; Moortgat, G. K.; Perner, D.; Poulet, G.; Restelli, G.; Sidebottom, H. *Atmos. Environ.* **1991**, *25A*, 1.
(17) Sabljic, A.; Güsten, H. *Atmos. Environ.* **1990**, *24A*, 73.
(18) De More, W. B.; Sander, S. P.; Golden, D. M.; Hampson, R. F.; Kurylo, M. J.; Howard, C. J.; Ravishankara, A. R.; Kolb, C. E.; Molina, M. J. *NASA Panel for Data Evaluation*; 1997.
(19) Wallington, T. J.; Hurley, M. D.; Fracheboud, J. M.; Orlando, J. J.; Tyndall, G. S.; Sehested, J.; Mogelberg, T. E.; Nielsen, O. J. *J. Phys. Chem.* **1996**, *100*, 18116.
(20) Mogelberg, T. E.; Sehested, J.; Tyndall, G. S.; Orlando, J. J.; Fracheboud, J. M.; Wallington, T. J. *J. Phys. Chem. A* **1997**, *101*, 2828.
(21) Picquet-Varrault, B.; Doussin, J. F.; Durand-Jolibois, R.; Carlier, P. *J. Phys. Chem. A* **2002**, *106*, 2895.

Received for review January 23, 2002. Revised manuscript received July 9, 2002. Accepted July 10, 2002.

ES0200138